

## Supplementary Information

### **Enhancing electro-codeposition and electrocatalytic properties of poly(neutral red) and FAD to determine NADH and H<sub>2</sub>O<sub>2</sub> using amino-functionalized multi-walled carbon nanotubes**

Kuo Chiang Lin, Jia Yan Huang and Shen Ming Chen\*

Electroanalysis and Bioelectrochemistry Lab, Department of Chemical Engineering and Biotechnology, National Taipei University of Technology, No.1, Section 3, Chung-Hsiao East Road, Taipei 106, Taiwan.

†Electronic Supplementary Information (ESI) available: [details of any supplementary information available should be included here]. See DOI: 10.1039/b000000x/

*Preparation of the PNR-FAD-MWCNT modified electrode*

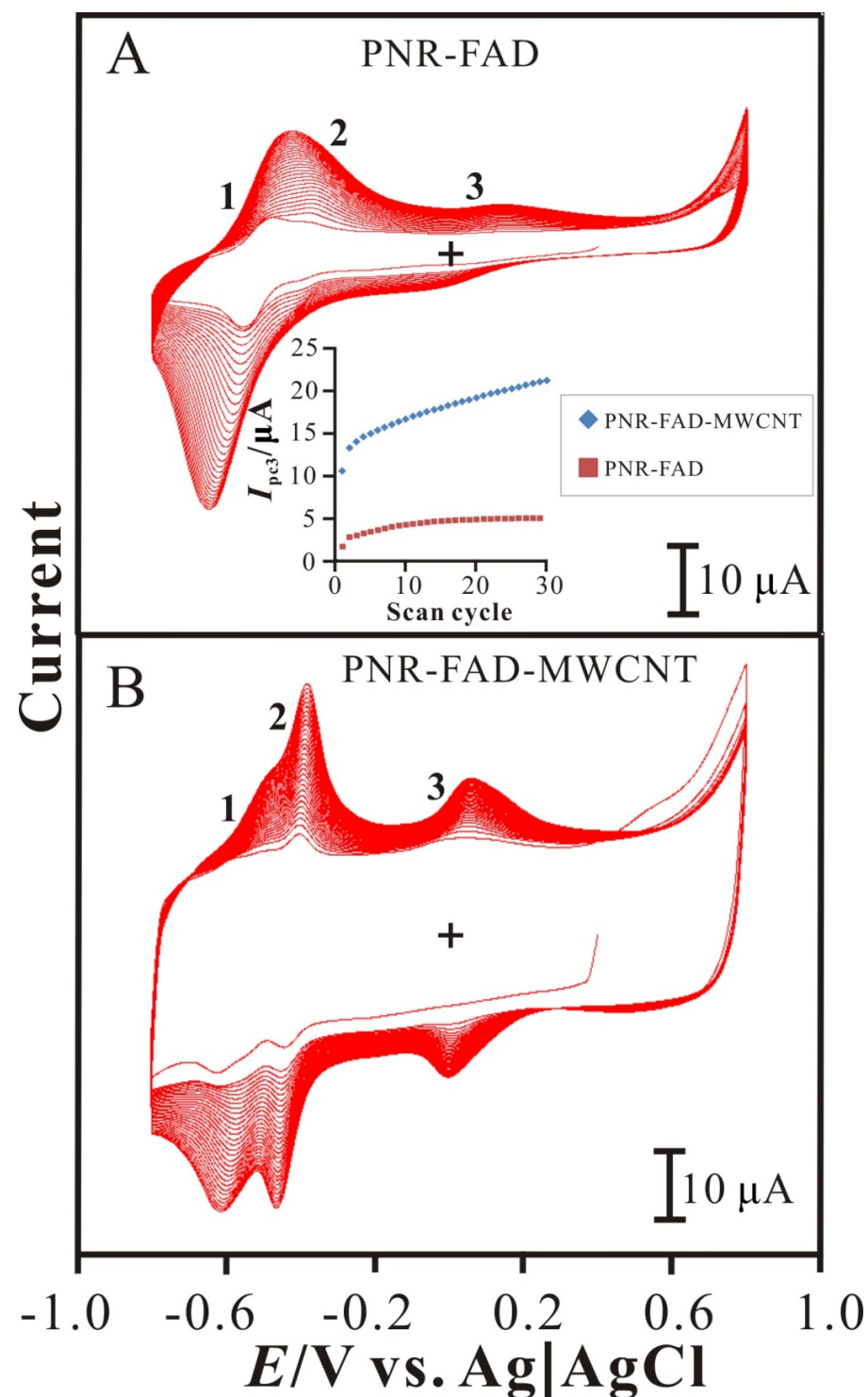
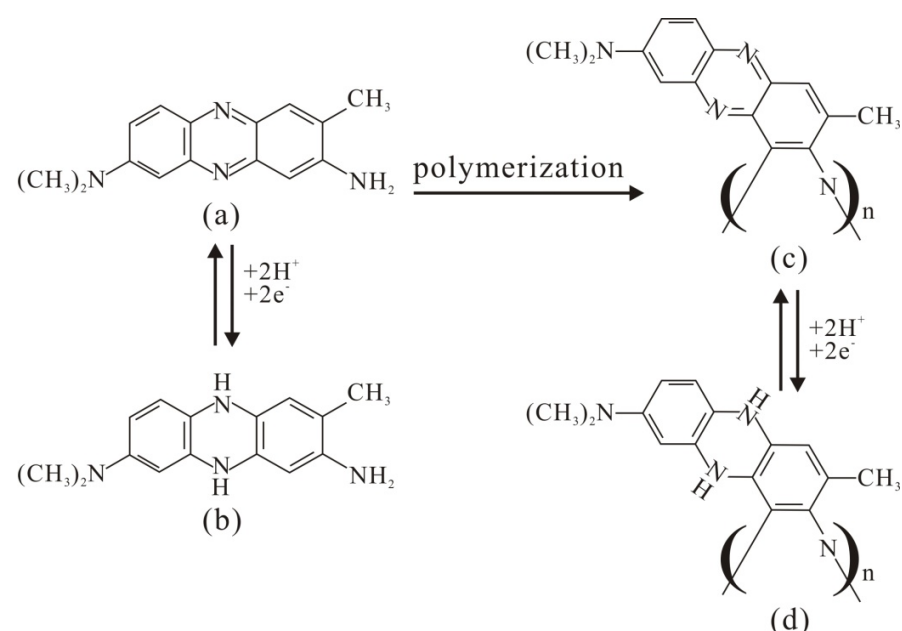


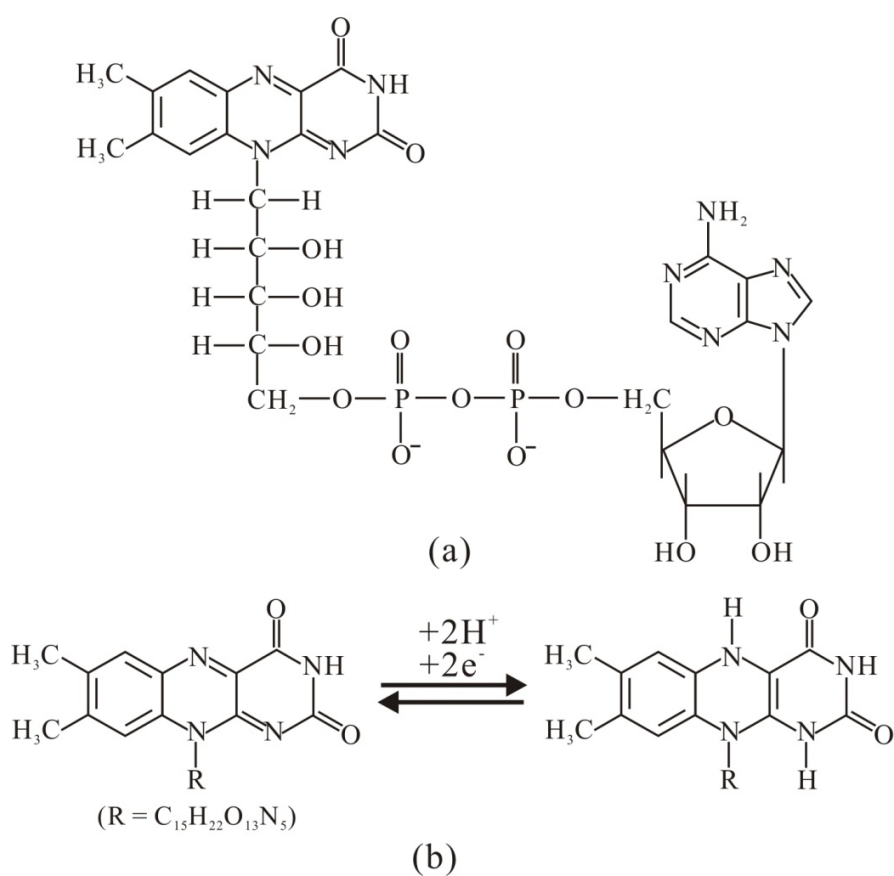
**Figure S1** CVs of (A) GCE and (B) MWCNT/GCE examined in pH 7 PBS containing  $10^{-4}$  M NR and  $10^{-5}$  M FAD. Scan rate =  $0.1 \text{ Vs}^{-1}$ . Inset: the plot of  $I_{pc3}$  vs. scan cycle.

Neutral red (NR) a phenazine redox dye, with an amino group located on heteroaromatic phenazine ring, makes it amenable to facilitate electropolymerization. **Scheme S1** shows the structure and redox process of neutral red and poly(neutral red) (PNR). The protonation and polymer film formation of neutral red can be expressed by case (a)-(d).



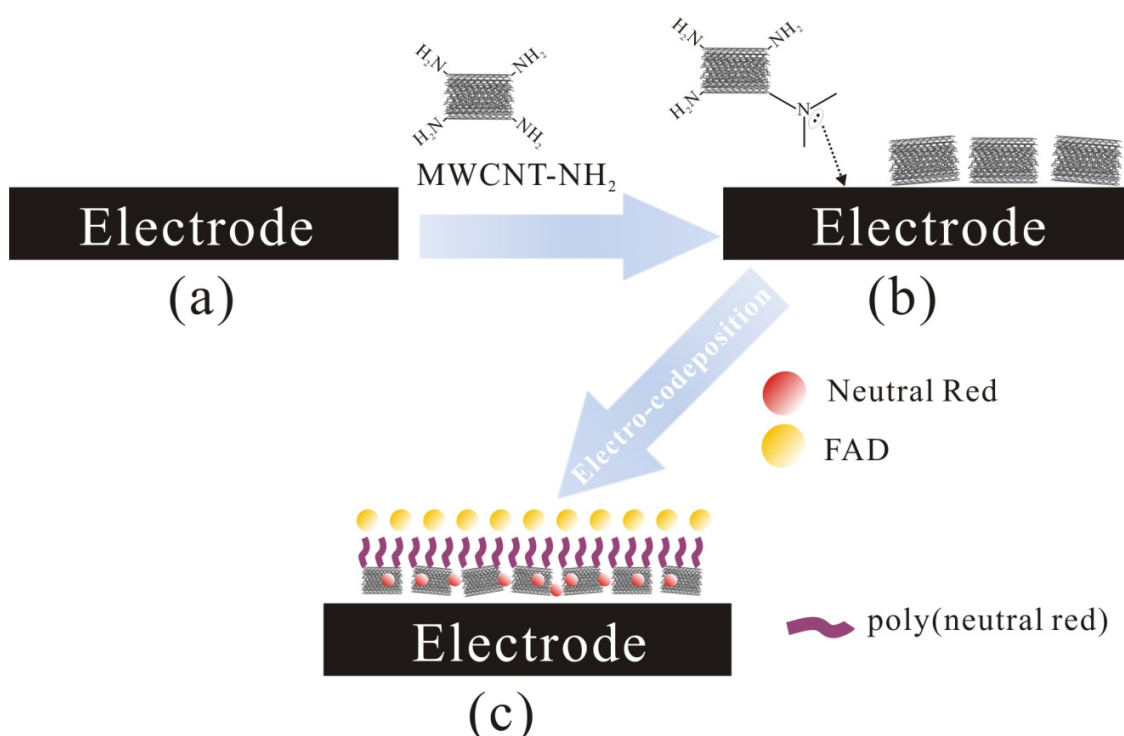
**Scheme S1** Illustration of the structure and redox process of neutral red (a & b) and poly(neutral red) (c & d).

Flavin adenine dinucleotide (FAD) is a flavoprotein coenzyme that plays an important biological role in many oxidoreductases and in reversible redox conversions in biochemical reactions. As shown in **Scheme S2**, it consists of the nucleotide adenine, the sugar ribose, and two phosphate groups. FAD and  $\text{FADH}_2$  have an isoalloxazine ring as the redox-active component that readily accepts and donates electrons. This makes it ideally suited to be an intermediate that is cyclically reduced and then re-oxidized by the metabolic reactions.



**Scheme S2** Structure and redox process of flavin adenine dinucleotide (FAD).

The PNR-FAD-MWCNT modified electrode can be easily prepared as shown in **Scheme S3**. The amino-functionalized MWCNT adsorb on electrode surface due to its long pair attractive to the electrode surface. When this electrode is transferred to the neutral solution in the presence of NR and FAD, some NR monomers are firstly initiated to be oxidized form and further electropolymerized with suitable positive potential control. By the way, the negative charged FAD is attracted by the positive PNR and codeposited on electrode surface. In contrast, these active materials are easily prepared in this procedure and it shows better voltammetric response than those using MWCNT (without functionalized group) or carboxyl-functionalized MWCNT. It provides the reason for the suitable preparation of hybrid nanocomposites. Therefore, the amino-functionalized MWCNT is used to study in whole work.



**Scheme S3** Experimental procedure of PNR-FAD-MWCNT hybrid composite: (a) bare electrode, (b) amino-functionalized MWCNT immobilized on electrode, and (c) electropolymerization of neutral red inducing FAD codepositon on MWCNT-electrode.

*Electrochemical impedance spectroscopic measurements and equivalent circuit model of PNR-FAD-MWCNT*

The electrochemical impedance spectroscopy (EIS) can give information on the impedance changes of the electrode surface during the modification process (Wilson and Turner, 1992). EIS spectra can provide the semicircle arc at higher frequencies correspond to the electron transfer limited process or the electron transfer resistance ( $R_{et}$ ). The linear segment at lower frequencies shows a diffusion controlled process. **Figure S2A** displays the Nyquist plots of the impedance spectroscopy for different composite modified electrodes including (a) bare, (b) PNR, (c) MWCNT, (d) PNR-FAD-MWCNT, and (e) PNR-MWCNT modified GCE examined in pH 7 PBS containing  $5 \times 10^{-3}$  M  $\text{Fe}(\text{CN})_6^{3-/4-}$ . Curve (a) shows the EIS spectra of the bare GCE which exhibits a straight line and a large semicircle arc ( $R_{et} = 368.3 \Omega$ ). Curve (b)-(e) individually depicts a straight line with a

smaller depressed semicircle arc estimated in  $R_{et} = 292.8 \Omega$ ,  $57.1 \Omega$ ,  $55.5 \Omega$ , and  $17.5 \Omega$  for PNR/GCE, MWCNT/GCE, PNR-FAD-MWCNT/GCE, and PNR-MWCNT/GCE, respectively. One can know that the modified electrodes exhibit lower electron transfer resistance than that of bare GCE. This phenomenon indicates that the electroactive species effectively altering the activity on electrode surface. Particularly, the PNR-MWCNT/GCE shows low resistance which is even lower than that of MWCNT/GCE. This result implies that the PNR deposition on amino-MWCNT might involve the amino-carbon linkage between amino-MWCNT and PNR polymer chain resulted in the conductive conjugated structure. As the result, the hybrid composite can show high current response and low electron transfer resistance.

Considering the location of MWCNT in this hybrid composite is also one important information, the MWCNT/PNR-FAD is marked for another hybrid type which means that the hybrid composite is prepared through the procedure with first PNR-FAD electropolymerization and then MWCNT adsorption. The FAD/GCE and MWCNT/PNR-FAD/GCE was further tested and compared to understand how the resistance change caused by modifiers and MWCNT location in the hybrid composite. **Figure S2B** shows the EI spectra for (a) FAD/GCE ( $R_{et} = 520.4 \Omega$ ), (b) MWCNT/PNR-FAD/GCE ( $R_{et} = 327.1 \Omega$ ), and (c) PNR-FAD-MWCNT/GCE ( $R_{et} = 55.5 \Omega$ ), respectively. One can know that FAD has higher electron transfer resistance and the resistance can be lowered in the presence of PNR and MWCNT. One can also know that the suitable MWCNT location in the hybrid composite should be immobilized before PNR and FAD electrocodeposition. This result might provide the evidence that the active hybrid composite contains amino-carbon linkage between amino-MWCNT and PNR polymer chain. As a result, the interfacial electron transfer resistance gradually decreased in their values upon the immobilization of PNR, PNR-FAD, and PNR-FAD-MWCNT. These data show that the PNR-FAD-MWCNT composite was successfully attached on the electrode surface to form an electroactive and compact structure.

In order to understand the impedance diagrams in the whole frequency range, the equivalent circuit model was proposed for PNR-FAD-MWCNT hybrid composite as shown in **Scheme S4**. It presents an equivalent circuit model simulated to fit the Nyquist plot of PNR-FAD-MWCNT with less error (mean error = 0.9%). The high frequency

response corresponded to the electrical behavior of the PNR-FAD-MWCNT and the low frequency impedance was attributed to the electrochemical kinetic of the diffusion. By the result, it provides the solution resistance ( $R_s$ ) of 187.5  $\Omega$ , the electron transfer resistance ( $R_{et}$ ) of 34.49  $\Omega$ , the diffusion impedance ( $W_0$ ) of 1.96 kDW, and the double layer capacitance ( $C$ ) of 177.8  $\mu\text{F}$ , respectively. One can know that the hybrid composite does lower the electron transfer resistance in the electrode surface as compared to bare electrode and other modifiers except of PNR-MWCNT. The double layer capacitance can be also proved by the positively charged PNR and the negatively charged FAD in the equivalent circuit model. The goodness of fit is illustrated in the fitting of the impedance data for the PNR-MWCNT modified electrode exemplified in Fig. S2, verifying the feasibility of this equivalent circuit to adequately represent the electrochemical system.

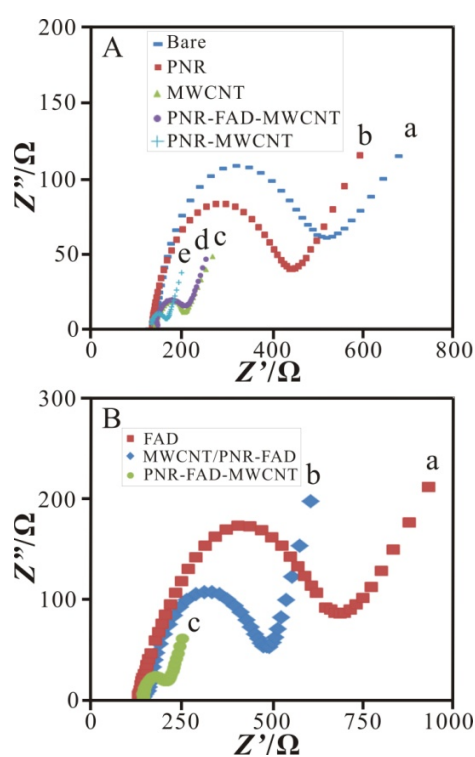
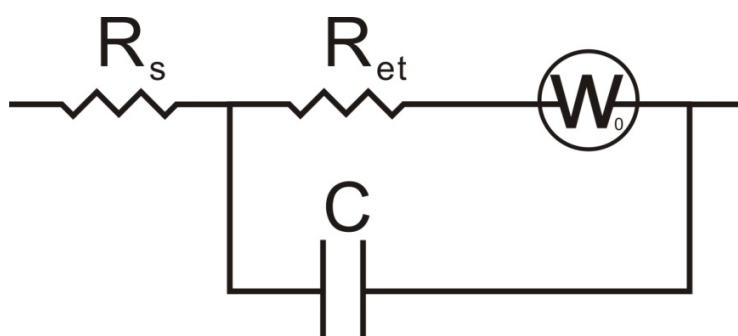


**Figure S2** (A) EIS spectra of (a) bare, (b) PNR, (c) MWCNT, (d) PNR-FAD-MWCNT, and (e) PNR-MWCNT modified GCE examined in pH 7 PBS containing  $5 \times 10^{-3}$  M  $\text{K}_3\text{Fe}(\text{CN})_6$ . (B) EIS spectra of (a) FAD, (b) MWCNT/PNR-FAD, and (c) PNR-FAD-MWCNT modified GCE examined in pH 7 PBS containing  $5 \times 10^{-3}$  M  $\text{Fe}(\text{CN})_6^{3-/-4-}$ .



**Scheme S4** Equivalent circuit used to fit the experimental impedance data of PNR-FAD-MWCNT in Fig. S2.

#### *Hydrodynamic voltammograms of PNR-FAD-MWCNT film for NADH and H<sub>2</sub>O<sub>2</sub>*

In order to understand the reaction mechanisms and evaluate the rate constants, the hybrid composite was immobilized on rotating disk electrode to study the electrocatalytic reactions by hydrodynamic voltammetry. **Figure S3** shows the voltammograms of PNR-FAD-MWCNT examined with NADH and H<sub>2</sub>O<sub>2</sub>, respectively. **Fig. S3A** shows the voltammograms of PNR-FAD-MWCNT modified rotating disk electrode examined at various NADH concentrations of  $1 \times 10^{-4} - 1 \times 10^{-3}$  M. Inset of **Fig. S3A** shows the Levich plots obtained by PNR-FAD-MWCNT/GCE for five different NADH concentrations (rotation speed  $\omega = 2500$  rpm). **Fig. S3B** shows the voltammograms of PNR-FAD-MWCNT modified rotating disk electrode examined at various rotation speed ( $\omega = 200 - 2500$  rpm) in the presence of  $5 \times 10^{-3}$  M H<sub>2</sub>O<sub>2</sub>. Inset of **Fig. S3B** shows the Levich plots obtained by PNR-FAD-MWCNT/GCE for five different H<sub>2</sub>O<sub>2</sub> concentrations (rotation speed  $\omega = 2500$  rpm).

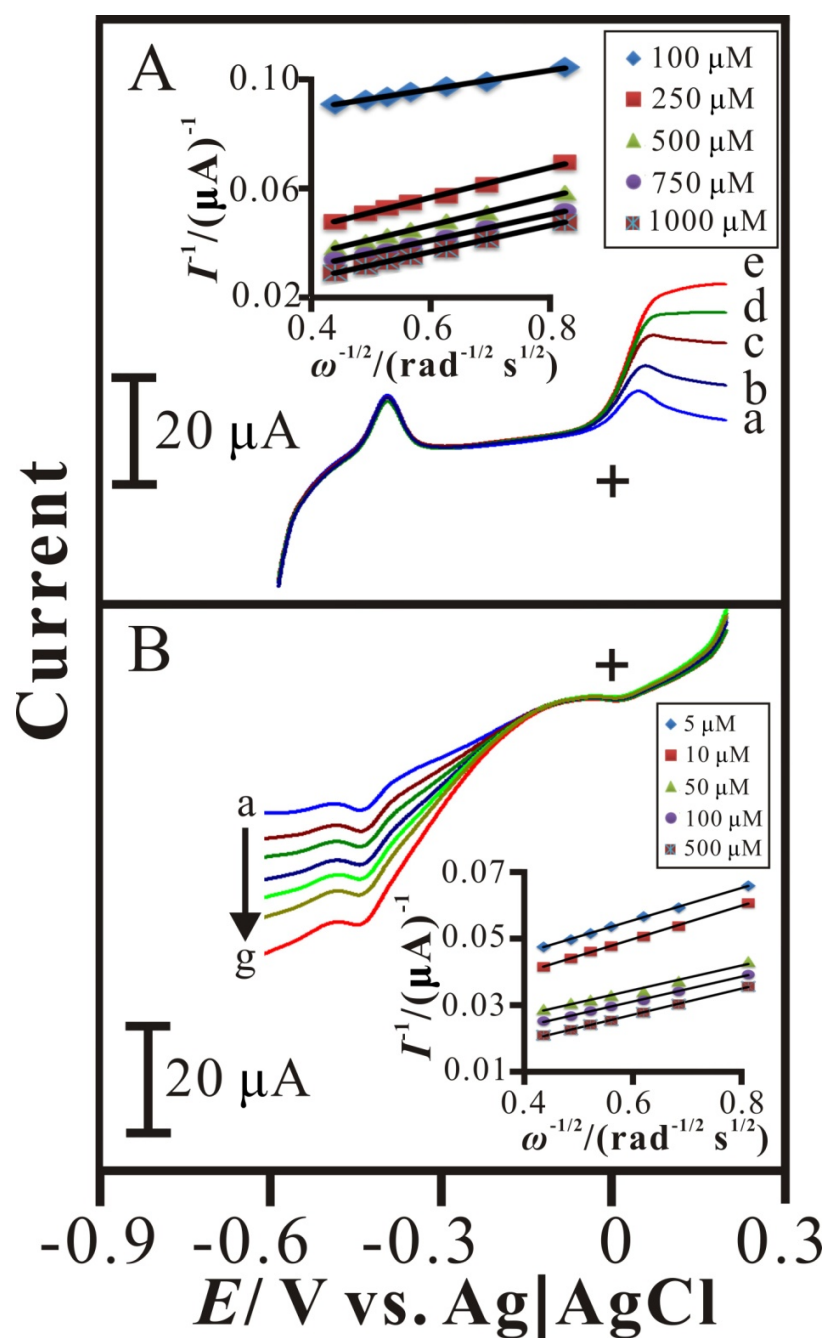


**Figure S3** RDE voltammograms of PNR-FAD-MWCNT/GCE examined in pH 7PBS containing (A)  $[\text{NADH}] = (\text{a}) 1 \times 10^{-4} \text{ M}, (\text{b}) 2.5 \times 10^{-4} \text{ M}, (\text{c}) 5 \times 10^{-4} \text{ M}, (\text{d}) 7.5 \times 10^{-4} \text{ M}$ , and (e)  $1 \times 10^{-3} \text{ M}$  ( $\omega = 2500 \text{ rpm}$ ); (B)  $[\text{H}_2\text{O}_2] = 5 \times 10^{-3} \text{ M}$  ( $\omega = (\text{a}) 200 \text{ rpm} - (\text{g}) 2500 \text{ rpm}$ ), respectively. Scan rate =  $0.015 \text{ Vs}^{-1}$ . Insets: the plots of  $I^1$  vs.  $\omega^{-1/2}$ .